# Study of the effects of proteasome inhibitors on ribosomal protein S19 (RPS19) mutants, identified in patients with Diamond-Blackfan anemia

Aurore Crétien,[1,2] Corinne Hurtaud,[1,2] Hélène Moniz,[1,2] Alexis Proust,[3] Isabelle Marie,[3,4] Orianne Wagner-Ballon,[1,2,5] Valérie Choesmel,[6,7] Pierre-Emmanuel Gleizes,[6,7] Thierry Leblanc,[4,8] Jean Delaunay,[3,4] Gil Tchernia,[4] Narla Mohandas,[9] and Lydie Da Costa[1,4,10]

[1]INSERM U790, Villejuif, France; [2]Univ Paris-Sud, Villejuif, France; [3]AP-HP, Hôpital de Bicêtre, Le Kremlin-Bicêtre, France; [4]Centre de référence des maladies génétiques de l'érythrocyte et de l'érythropoïèse, Hôpital Bicêtre, Université Paris XI, Le Kremlin-Bicêtre, France; [5]AP-HP, Hôpital Henri-Mondor, Créteil, France; [6]Université Paul Sabatier, Laboratoire de Biologie Moléculaire des Eucaryotes, Toulouse, France; [7]CNRS, UMR5099, Toulouse, France; [8]AP-HP, Hôpital Saint-Louis, Paris, France; [9]New York Blood Center, New York, NY, USA, and [10]AP-HP, Hôpital Robert-Debré, Paris, France

## ABSTRACT

### Background

Mutations in the ribosomal protein S19 gene (*RPS19*) have been found in 25% of patients with Diamond-Blackfan anemia, a rare syndrome of congenital bone marrow failure characterized by erythroblastopenia and various malformations. Mechanistic understanding of the role of RPS19 in normal erythropoiesis and in the Diamond-Blackfan anemia defect is still poor. However, defective ribosome biogenesis and, in particular, impaired 18S ribosomal RNA maturation have been documented in association with various identified *RPS19* mutations. Recently, new genes, all encoding ribosomal proteins, have been found to be mutated in Diamond-Blackfan anemia, adding further support to the concept that ribosome biogenesis plays an important role in regulating erythropoiesis. We previously showed variability in the levels of expression and subcellular localization of a subset of RPS19 mutant proteins.

### Design and Methods

To define the mechanistic basis for this variability better, we studied a large number of mutant proteins and characterized both RPS19 expression level using a specific antibody against RPS19 and RPS19 subcellular localization after transfection of Cos-7 cells with various green fluorescent protein-RPS19 mutants. To investigate the role of the proteasome in RPS19 degradation, we examined the effect of various proteasome inhibitors, namely lactacystin, MG132, and bortezomib on RPS19 expression and subcellular localization

### Results

We found two distinct classes of RPS19 protein defects in Diamond-Blackfan anemia based on the stability of the mutant proteins: (i) slightly decreased to normal levels of expression and normal nucleolar localization and (ii) markedly deficient expression and failure to localize to the nucleolus. All the proteasome inhibitors tested were able to restore the expression levels and normal subcellular localization of several unstable mutant proteins.

### Conclusions

Our findings demonstrate an important role for the proteasomal degradation pathway in regulating the expression levels and nucleolar localization of certain mutant RPS19 proteins in Diamond-Blackfan anemia.

Key words: RPS19, Diamond-Blackfan anemia, nucleolar localization, proteasome inhibitors, bortezomib.

*Citation: Crétien A, Hurtaud C, Moniz H, Proust A, Marie I, Wagner-Ballon O, Choesmel V, Gleizes P-E, Leblanc T, Delaunay J, Tchernia G, Mohandas N, and Da Costa L. Study of the effects of proteasome inhibitors on ribosomal protein S19 (RPS19) mutants, identified in patients with Diamond-Blackfan anemia. Haematologica 2008; 93:1627-1634. doi: 10.3324/haematol.13023*



*Acknowledgments: we are very grateful to Dr. William Vainchenker for fruitful discussions, to Dr. S. Giraudier for constructive discussions, to Yann Lecluse for his help in cytometry experiments, and to Dr. Claire Lacombe-Sourdot (CNRS-Université Paris-6, Institut Jacques Monod) for providing us the Cos-7 cell line. We would like to acknowledge the patients and their families for their cooperation, our collaborators taking care of the German, Italian, and American registries, and the members of SHIP.*

*Funding: this work was supported by the Institut National de la Santé et de la Recherche Médicale (INSERM), France, NIH grant HL079565, the ANR (RIBODBA project), the DBA Foundation and the Daniella Maria Arturi Foundation, USA.*

*Manuscript received March 6, 2008. Revised version arrived May 26, 2008. Manuscript accepted June 23, 2008.*

*Correspondence:*
*Lydie Da Costa, MD, PHD, Service d'Hématologie biologique, Hôpital Robert Debré, 48 boulevard Sérurier, 75019 Paris, France.*
*E-mail: lydiedacosta@free.fr/ lydie.dacosta@rdb.aphp.fr*

## Introduction

Diamond Blackfan anemia (DBA)[1,2] is a rare congenital erythroblastopenia associated with a heterogeneous phenotype. DBA is usually diagnosed early in infancy on the basis of anemia and the absence or marked reduction of erythroid precursors in an otherwise normocellular bone marrow. Around 40% of DBA patients exhibit various malformations, mostly in the cephalic area.[3] The ribosomal protein S19 gene (*RPS19*), encoding a ribosomal protein (S19), which is located in the beak of the small ribosomal subunit 40S of the ribosome,[4] was the first gene identified to be involved in DBA.[5] Mutations in *RPS24* and *RPS17* genes have also been described in a few DBA patients.[6,7] Recently, mutations in additional ribosomal protein encoding genes have been identified in association with DBA.[8,9] Taken together these findings show that mutations in ribosomal genes account for the DBA phenotype in at least 46% of patients. All individuals are heterozygous suggesting that homozygosity is likely to be lethal.[5,10-12]

A *hot spot* of *RPS19* gene mutations is located between codon 52 and codon 62.[10] No correlation between the genotype and the clinical presentation has been established. The molecular mechanisms by which RPS19 mutations cause blockade of erythropoiesis have yet to be defined. Unfortunately, animal models have thus far failed to provide significant insights into this problem. Homozygous knock-out RPS19$^{-/-}$ mice died *in utero* while heterozygote RPS19$^{+/-}$ mice did not exhibit any hematologic or other abnormalities.[13] However, knock- down of RPS19 in human bone marrow or cord blood CD34$^{+}$ cells using siRNA-lentivirus reproduced the blockade in erythroid cell proliferation and differentiation observed in DBA[14] implying that RPS19 plays a functional role in regulating erythropoiesis. Importantly, some recent studies characterized DBA as a disease of ribosome biogenesis and, specifically, of maturation of the pre40S subunit.[15-18]

We previously showed that both endogenous and green fluorescence protein (GFP)-fused RPS19 localize to the nucleoli of Cos-7 fibroblasts.[19] We also reported variability in the levels of expression and subcellular localization of a subset of RPS19 mutant proteins. To better define the mechanistic basis of this variability, in the present study, we examined the expression levels and nucleolar localization of a large number of mutant RPS19 proteins.

## Design and Methods

### Description of the patients with Diamond-Blackfan anemia carrying RPS19 gene mutations

Thirteen DBA patients from unrelated families from France, Germany and Italy were studied. The RPS19 protein mutations and the clinical data detailing the phenotypes of these patients are shown in Table 1. The *RPS19* gene mutations chosen for the study correspond to the well known variability of mutations identified in the disease. Informed consent to participation in this investigation was obtained from either the patients or their parents.

**Table 1.** Description of the 13 patients affected by Diamond-Blackfan anemia.

| *Probands* | *RPS19 gene mutation* | *Age at diagnosis (months)* | *Sex* | *Hb count at diagnosis (g/L)* | *Reticulocyte count at diagnosis ($10^9$/L)* | *Malformations* | *Treatment at the time of study* |
|---|---|---|---|---|---|---|---|
| 1 | Trp52Cys | 8.4 | M | 30 | 3.00 | Low hair implantation | Treatment independence |
| 2 | 24del18 deletion of aa 9 to 14 | Post mortem | F | 75 | 5.88 | None | T and death |
| 3 | Gly120Ser | 2 | F | 50 | Less than 20.00 | None | T |
| 4 | Leu131Pro | 2 | F | 45 | 12.50 | SGA Short stature | T |
| 5 | InsAG36 stop in 29 | 6 | F | NA | NA | None | Treatment independence |
| 6 | InsG238 stop in 153 | 1 | M | NA | NA | None | Treatment independence |
| 7 | Trp33stop | 2 | M | NA | NA | Hydrocephalia Cerebral atrophia IAC Bone anomalies | T |
| 8 | Tyr48stop | 2 | F | 42 | 2.00 | Low implantation of the thumb | T |
| 9 | Arg56stop | 0.25 | M | 53 | 3.94 | Short stature | T and death |
| 10 | Met75stop | 1.9 | M | 37 | 3.00 | Low hair implantation | S |
| 11 | Arg94stop | 2 | M | 29 | NA | None | T |
| 12 | Ala100stop | 1.2 | F | 39 | 4.56 | Short stature | S |
| 13 | 390del2 stop in 151 | 11 | F | NA | NA | Severe congenital hypogammaglobulinemia | Treatment independence |

*F: female; M: male; SGA: small for gestational age; IAC, Interauricular communication; T: transfusion dependence; and S: steroid; NA: non available.*

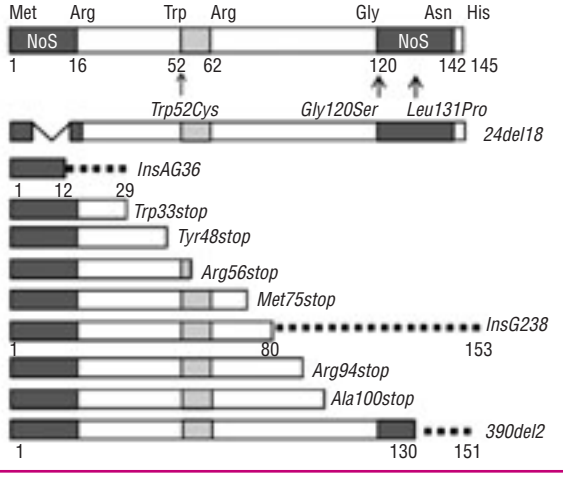


**Figure 1.** Representation of the patients' mutations: the RPS19 protein sequence is shown from the initiation methionine to the last amino acid, the histidine. The N-and C-termini described previously as *NoS* (nucleolar localization signal) are represented as dark gray boxes, encompassing the first 15 amino acids and the glycine 120 to the asparagine 142, respectively. The *hot spot* of mutations identified in Diamond-Blackfan anemia from the tryptophan 52 to the arginine 62 is shown as a light gray box. Arrows indicate the missense mutations studied: Trp52Cys, Gly120Ser, and Leu131Pro. The 24del18 mutation deletes amino acids 9 to 14 without any frameshift of the RPS19 protein sequence. InsAG36, InsG238, and 390del2 are responsible for a frameshift beginning with the amino acids, 12, 80 and 130, respectively, resulting in stop codons at amino acids 29, 153, and 151, respectively. All the nonsense mutations, Trp33stop, Try48stop, Arg56stop, Met75stop, Arg94stop, and Ala100stop lead to a premature stop codon and variously truncated RPS19. All the insertion and nonsense mutations suppress the entire C-terminal *NoS* and the 390Del2 mutation deletes amino acids 131 to 142 in this C-terminal region.

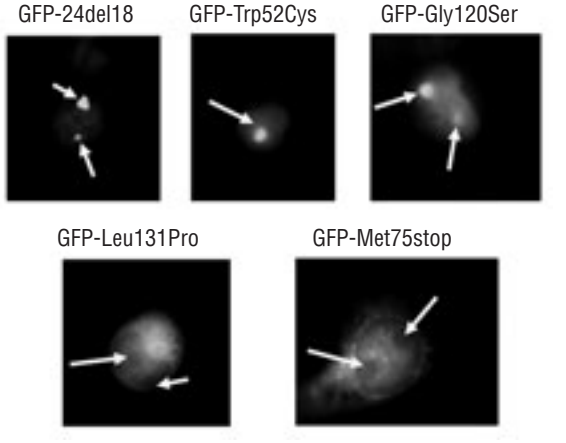


**Figure 2.** RPS19 nucleolar localization analyses: we analyzed the subcellular distribution of RPS19 after transfection of Cos-7 cells with GFP-wild type and various mutant RPS19. The figures shown here are merged fields of DAPI+FITC staining for GFP –24del18, –Trp52Cys, –Gly120Ser, Leu131Pro, –Met75stop RPS19 mutants. While GFP-24del18, –Trp52Cys, and –Gly120Ser RPS19 mutants localized in Cos-7 cell nucleoli, GFP-Leu131Pro and Met75stop failed to localize to the nucleoli. Arrows indicate the nucleoli in the cell. Original magnification: ×63.

### DNA cloning

Full length wild-type (WT) human and mutant RPS19 cDNA carrying specific mutations identified in DBA patients were cloned in frame into the pEGFP-C3 mammalian expression vector (BD Biosciences-Clontech Laboratories), which encodes a green fluorescent protein (Figure 1). All the RPS19 constructs, except 24del18 and Ala100stop, were generated by site-directed mutagenesis of the pEGFP-C3-WT RPS19 clone using a QuickChange mutagenesis kit (Stratagene). The two long deletions, 24del18 and Ala100stop, were generated by the splice overlap extension method. Information on various primers used is available on request. All pEGFP-C3 constructs were sequenced with an ABI Big Dye Terminator sequencing kit using an Applied Biosystems 373 DNA sequencer (Perkin Elmer).

### Cos-7 cell culture and transfection

Cos-7 cells were cultured and transfected as previously described.[19] Three independent experiments were performed with each mutant GFP-RPS19 and the findings compared with those of cells transfected with GFP-wild type RPS19 and non-transfected cells.

### Immunoprecipitation

Cos-7 cells from culture dishes were washed twice with phosphate-buffered saline (PBS) 12 to 18 h after transfection. The lysis buffer was added to the dish. After 30 min of cell lysis on ice, the cell suspension was centrifuged and then 100 μL of protein G agarose beads were added to the supernatant for 1 h for pre-clearing at 4°C. Following centrifugation, the supernatant was mixed with the agarose beads coupled to 5-10 μg of specific rabbit IgG antibody against ubiquitin (Calbiochem) and incubated overnight at 4°C. After centrifugation and washes, the beads were suspended in 100 μL of 2X SDS-PAGE denaturing buffer and dithiothreitol (DTT). The samples were boiled for 10 min and stored at -80°C until western blot analyses could be performed.

### Immunoblotting

Cos-7 cells were immunoblotted as previously described.[19] The membrane with transferred proteins was incubated with an antibody against RPS19 or an antibody against actin (clone C4) (ICN Biomedicals) or an antibody against GFP (Roche) diluted at 1:1000 or an antibody against histone deacetylase 1 (HDAC1) (Santa Cruz Biotech) diluted at 1:500. The antibodies against RPS19 and actin were used at the concentrations previously described.[19] The specific protein band was revealed by secondary antibodies coupled with horseradish peroxidase.[19] A goat anti-rabbit antibody (Vector labs) was diluted 1:1000 for the detection of HDAC1.

### Immunofluorescence microscopy

Cos-7 cells, either untransfected or transfected with pEGFP-C3 constructs, were processed as previously described[19] and viewed using an Eclipse E600 inverted microscope (Nikon, Kanagawa, Japan). Images were acquired using CoolSNAP 1.2 software (Roper Scientific, Inc.). We analyzed the distribution of GFP-RPS19 fusion proteins in different subcellular compartments by counting the percentage of cells exhibiting staining in the different compartments: the nucleus, the

cytoplasm, and nucleoli. Nucleolar localization was evaluated in 200 transfected cells and three independent transfections were carried out with each construct.

### Proteasome inhibition

The proteasome of Cos-7 cells was inhibited by classic proteasome inhibitors: lactacystin, MG132 (Calbiochem) or bortezomib (Janssen-Cilag, Millennium). Cells were incubated in the DMEM culture medium with lactacystin or MG132 at 10 μmol/L or bortezomib at 2.5 ng/mL for 8 hours and then transfected with various RPS19 constructs. Twelve hours after transfection, cells were collected for immunoblot or immunofluorescence analysis.

### Cell fractionation

After treatment of Cos-7 cells with or without bortezomib and transfection with GFP-wild type or mutant RPS19, the cells were treated for 10 min with 100 μg/mL cycloheximide. Cell fractionation was then performed as previously described.[20]

## Results

### RPS19 mutations located in the hot spot (codon 52), 24Del18 and Gly120Ser mutants exhibit a slightly decreased to normal levels of expression and normal nucleolar localization of RPS19

The various RPS19 mutations explored in the present study are shown in Figure 1. As previously described,[19] human WT RPS19 fused to GFP localized to the nucleoli, while GFP alone was found exclusively in the cytoplasm (*data not shown*). The Trp52Cys hot spot RPS19 mutant exhibited normal nucleolar localization (Figure 2). Quantification of the cellular localization of the mutant protein showed nucleolar localization in 66% of transfected cells (Figure 3). Furthermore, the level of expression of this mutant protein (Figure 4, Panel A, lane 6) was between 70 to 100% of that of the wild type RPS19 (Figure 4, Panel A, lane 2). This finding is similar to our previous findings with other hot spot mutations: Arg62Trp, Arg56Gln, and Thr55Met.[19]

Two other mutations not located in the hot spot, 24Del18, which deletes amino acids 9 to 14 without a frameshift, and the mutation Gly120Ser located in the C-terminal region, also exhibited normal nucleolar localization (Figure 2). Quantification of the cellular localization of the mutant protein showed nucleolar localization in 62% of transfected cells for 24del18 and in 93% for Gly120Ser (Figure 3). The expression levels of these two mutant proteins were decreased compared to the expression of wild type protein but not to the same extent, as was the case for some other RPS19 mutants (Figure 4).

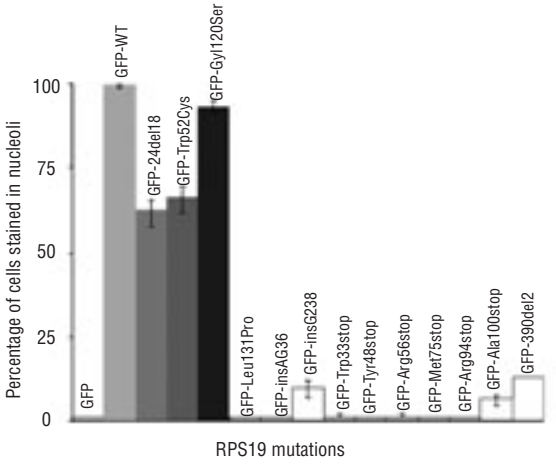


**Figure 3.** Analysis of the subcellular distribution of various mutant RPS19 fused to GFP in transfected Cos-7 cells: the nucleolar partitioning of 13 mutant RPS19 fused to GFP was compared with that of human WT RPS19. The percentage of cells showing nucleolar localization was quantified by examining 200 transfected cells from each transfection. The data shown are averages from three independent experiments.

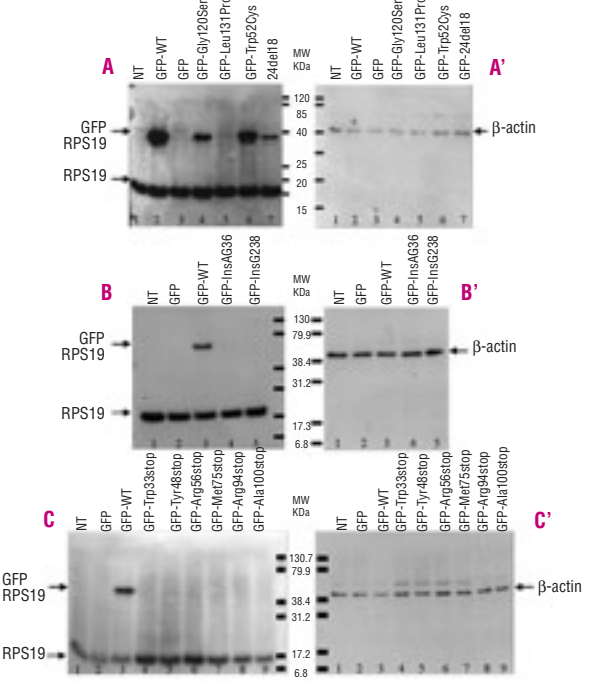


**Figure 4.** Differences in levels of expression of normal and mutant RPS19 proteins: lysates of Cos-7 cells transfected with different GFP fusion protein constructs including GFP alone, GFP-WT RPS19, and GFP-mutant RPS19-Gly120Ser, -Leu131Pro, -Trp52Cys and -24del18 (A), GFP-mutant RPS19-insAG36, and -insG238 (B), GFP-mutant RPS19 -Trp33stop, -Tyr48stop, -Arg56stop, -Met75stop, -Arg94stop, and -Ala100stop (C). Immunoblots were probed with a chicken polyclonal anti-RPS19 antibody (0.05 μg./L). The Leu131Pro, insAG36, insG238 and all the nonsense mutations tested, which impaired RPS19 nucleolar import, were consistently associated with a dramatic decrease in RPS19 expression (panel A, lane 5; panel B lanes 4-5; panel C, lanes 4-9). Endogenous RPS19 shown at the bottom of the membranes, confirms the equivalent amount of total proteins loaded into each lane. Western blots with an antibody against human β-actin (A', B' and C') also confirmed equivalent amounts of protein loading. Molecular weight standards are shown at the side of the blots.

### *Some RPS19 mutations result in dramatically reduced levels of protein expression and abnormal subcellular localization*

The Leu131Pro mutant failed to localize to the nucleoli and was present predominantly in the cell cytoplasm (Figure 2). We noted nucleolar localization in less than 1% of transfected cells (Figure 3). Importantly, western blot analysis showed a dramatic decrease in the level of expression of Leu131Pro mutant RPS19 (Figure 4, Panel A, lanes 4-5). Altered subcellular localization and a marked decrease in levels of protein expression were also features of nine other premature stop codon mutations that led to the deletion of varying lengths of the C-terminal region of the protein. In six cases, nonsense mutations led to premature termination (Trp33stop, Tyr48stop, Arg56stop, Met75stop, Arg94stop, Ala100stop). In two cases, insertions and in one case, a deletion led to a change in the reading frame resulting in a truncated protein, with altered C-termini. In all these nine cases, there was a significant failure of the mutant proteins to localize to the nucleoli (Figures 2 and 3), with nucleolar localization ranging from less than 1% in six cases to 7, 10, and 13%, in the other three. Importantly, the levels of expression of these nine mutant proteins were dramatically reduced compared to the expression of wild type protein. No mutant protein could be detected in the western blots for any of these nine mutants (Figure 4).

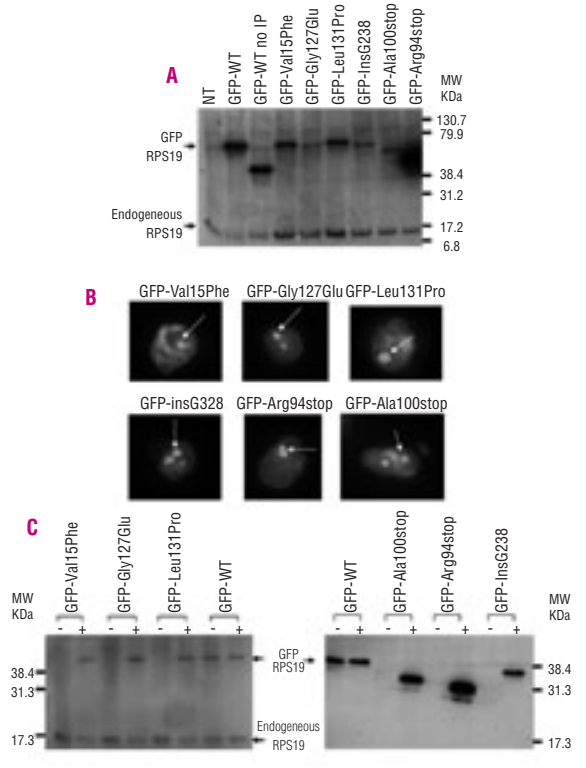


**Figure 5.** (A) RPS19 is an ubiquinated protein: transfection of Cos-7 cells with GFP wild type and mutant RPS19 followed by immunoprecipitation with an antibody against ubiquitin and immunoblotting with the anti-RPS19 antibody showed the ubiquination of endogenous, GFP-wild type and various RPS19 mutants. NT: non-transfected cells; GFP-WT: GFP-wild type; GFP-mutant RPS19: GFP-Val15Phe, -Leu131Pro, -Gly127Glu, -InsG238, -Ala100stop, -Arg94stop. The GFP-WT no IP lane shows RPS19 staining after transfection of GFP-WT but without ubiquitin immunoprecipitation. Molecular weight standards (MW) are shown at the side of the blots. (B) Effects of lactacystin on RPS19 nucleolar localization: the merged fields of DAPI+FITC staining for GFP -Val15Phe, -Gly127Glu, -Leu131Pro, -insG238, -Arg94stop and -Ala100stop RPS19 mutants are shown. Lactacystin restored the localization of all the GFP-RPS19 mutants to the nucleoli. Similar results were obtained with MG132 (*data not shown*). Arrows indicate the nucleoli in the cell. Original magnification: ×63. (C) Effect of lactacystin on RPS19 expression levels: lactacystin treatment increased the levels of expression of all mutant proteins. Lanes marked (-) are without lactacystin and lanes marked with (+) are with lactacystin. Similar results were obtained with MG132 (*data not shown*). Molecular weight standards (MW) are shown at the side of the blots.

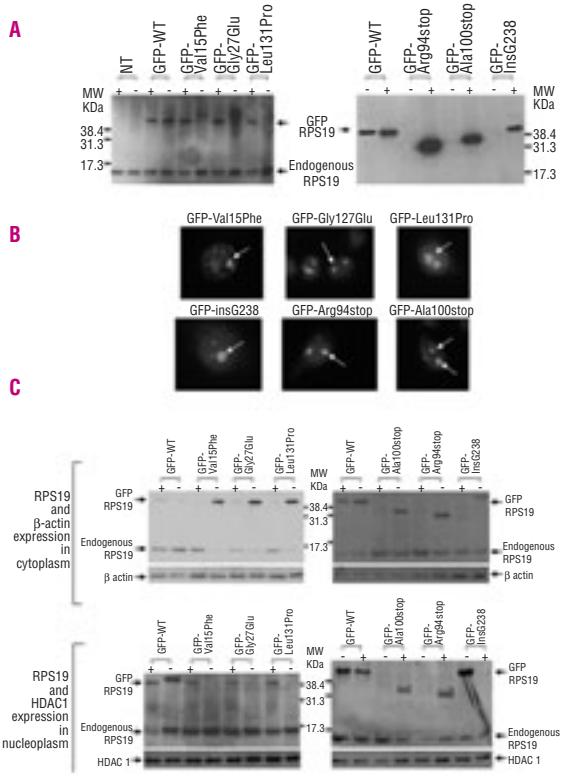


**Figure 6.** (A) Effects of bortezomib on RPS19 expression level: bortezomib treatment increased the levels of expression of all mutant proteins (GFP-Val15Phe-, -Gly127Glu-, -Leu131Pro-, -Ala100stop-, -Arg94stop-, and -insG238-RPS19). Lanes marked (-) are without bortezomib and lanes marked (+) are with bortezomib. Molecular weight standards (MW) are shown at the side of the blots. (B) Effects of bortezomib on RPS19 nucleolar localization; merged fields of DAPI+FITC staining for GFP -Val15Phe, -Gly127Glu, -Leu131Pro, -insG238, -Arg94stop and -Ala100stop RPS19 mutants are shown. Bortezomib restored the nucleolar localization of all the GFP-RPS19 mutants. Arrows indicate the nucleoli in the cell. Original magnifications x 63. (C) Cell fractionation with or without bortezomib: western blot analyses of the subcellular localization of GFP-WT and GFP-mutant RPS19 (GFP-Val15Phe, -Gly127Glu, -Leu131Pro, -Arg94stop, -Ala100stop, and -InsG238) after treatment of the cells with (+) or without bortezomib (-). The top two panels show cytoplasmic fractions and the bottom two panels show nucleoplasmic fractions. Histone deacetylase (HDAC1) was chosen as a nucleoplasm protein control. Bortezomib restored RPS19 nucleoplasmic localization in all the mutants tested.

### *The effect of proteasome inhibitors on expression levels and on nucleolar localization of mutant RPS19 proteins*

We documented that endogenous RPS19 as well as the wild type and mutant RPS19 proteins fused to GFP were ubiquitinated, a feature of most proteins targeted for proteasomal degradation (Figure 5A). We examined the ability of proteasome inhibitors to restore the expression levels of 15 RPS19 mutant proteins (13 identified in the present study and the two other that we had previously reported,[19] Val15Phe and Gly127Glu) (Table 1 and Figure 1). A key finding is that two different proteasome inhibitors restored the expression levels of seven of these mutant proteins, which were poorly expressed in Cos7 cells. The expression levels of Val15Phe, Gly127Glu, Leu131Pro and of truncated Arg94stop, Ala100stop, insG238 and 390del2 RPS19 were significantly higher following proteasome inhibition by lactacystin or MG132 (Figure 5C, *data not shown* for the 390del2 RPS19). In addition to restoring protein expression levels, the proteasome inhibitors also restored nucleolar localization of these seven mutant proteins (Figure 5B, *data not shown* for the 390del2 RPS19). In marked contrast, proteasome inhibition had no effect on either the expression or subcellular localization of truncated insAG36, Trp33stop, Tyr48stop, Arg56stop, and Met75stop RPS19 proteins (*data not shown*). Thus, proteasome inhibitors are effective in restoring both RPS19 protein expression levels and nucleolar localization as long as the truncated proteins contain more than 80 amino acids, but fail to do so when the mutated RPS19 contains less than 80 amino acids. It should be noted that the wild type RPS19 also undergoes proteasomal degradation but to a much lesser extent than the mutant proteins. This could be a reflection of the physiological degradation of wild type RPS19 in cells in steady state.

Bortezomib also restored RPS19 expression levels and nucleolar localization of all mutant proteins in which we found a beneficial effect with lactacystin and MG132 (Figure 6A and B). Following cell fractionation, we analyzed the subcellular partitioning (cytoplasm and nucleoplasm) of GFP-WT and mutant RPS19 in the presence and absence of bortezomib. As expected, in the absence of bortezomib the GFP-RPS19 mutants localized to the cytoplasmic fraction of the cells, while wild type RPS19 localized to the cell nucleoplasm (Figure 6C). Strikingly, in the presence of bortezomib the mutant RPS19 localized to the cell nucleoplasm (Figure 6C). This finding reinforces the major role played by proteasomal degradation in determining the fate of mutant RPS19 proteins.

## Discussion

The mechanisms underlying erythroblastopenia and morphogenetic abnormalities in DBA are still to be fully defined. However, some significant new insights have recently been gained. DBA has been shown to be a member of bone marrow failure syndromes, such as cartilage hair hypoplasia,[21-24] dyskeratosis congenita,[25,26] and Shwachman-Diamond syndrome,[17,27-29] in which ribosome biogenesis or RNA processing is impaired.[15,17,18]

In the present study, we identified two types of mutations in the *RPS19* gene, leading to two different phenotypes *in vitro*: (i) mutations associated with slightly decreased to normal levels of expression and a normal nucleolar localization and (ii) mutations which exhibit a dramatic decrease in RPS19 expression level and a significant alteration in nucleolar localization. The data presented here are in very good agreement with those of a recently published study of a large number of RPS19 missense mutants expressed in HEK293 cells.[30] In addition, we show that RPS19 proteins with premature stop codons are degraded by the proteasome, which indicates that nonsense-mediated decay is not the only mechanism operational in these mutants. The fact that proteasome inhibitors fail to stabilize RPS19 mutants with fewer than 80 amino acids may be due to major instability of these mutants, or because nonsense-mediated decay is more efficient for these short forms.

Recent elucidation of the crystal structure of the homolog of RPS19 in archeaon *Pyrococcus abyssi*[31] provides an explanation of these functional data. The mutations associated with a slight decrease in RPS19 expression levels and normal nucleolar localization are all accessible residues clustered within or around alpha helix 3 located in the central position in the structure and thereby impairing the function of the protein without altering its overall folding (class II mutations).[31] In contrast, mutations that exhibit a dramatic decrease in RPS19 expression levels alter structural residues affecting the folding of the protein and hence its stability (class I mutations).[31] Thus, our functional data show a remarkable correlation with RPS19 structure.

Another major finding of the present study is that impaired nucleolar localization and decreased expression of RPS19 are tightly linked. We suggest that these RPS19 mutants fail to localize into the nucleoli either because the mutation impairs their ability to translocate to the nucleoli and hence they are degraded or because the mutant protein is unstable and rapidly degraded by the proteasome. While we are unable to distinguish the relative contributions of these two mechanisms, our findings with proteasome inhibitors favor the second hypothesis since both RPS19 expression level and nucleolar localization are rapidly restored by proteasome inhibitors. These results imply that proteolysis of the mutant protein is a hallmark of these identified mutations. We previously described two regions involved in RPS19 nucleolar localization, one in the first 15 amino acids and the second one encompassing the Gly120 to the Asn 142 in the C-termini.[19] In the light of the data presented here, it is rather likely that deletion of either one of these domains induces protein instability, therefore hampering accumulation in the nucleolus.

The proteasome is predominantly localized in the cytoplasm but is also present in the nucleus. Recently, Lam *et al.*[32] showed proteasomal degradation of normal ribosomal proteins in the nucleus. We could thus

hypothesize that RPS19 mutants can be effectively translocated to the nucleolus and then degraded in the nucleoplasm. Further experiments using mass-spectrometry would be needed to define where exactly the proteasomal degradation of RPS19 mutants occurs in cells. Using mass-spectrometry-based organellar proteomics and stable isotope labeling, in yeast and HeLa cells, RPS19 was one of the first nucleolar proteins whose quantitative changes in response to metabolic inhibitors, including MG132, were analyzed.[32,33] RPS19 decreases two-fold in the nucleoli after actinomycin D treatment and increases two-fold in the nucleoli following MG132 treatment. It was suggested that there may be "a novel regulatory link between ribosome biogenesis and protein degradation pathways, acting to balance rates of protein synthesis and breakdown".[33] The understanding of the mechanisms that regulate the trafficking of RPS19 in and out of the nucleolus and the role of this protein in the regulation of cell proliferation and differentiation may provide important clues for understanding the pathophysiology of DBA.

The fact that protein levels of some of the mutants can be restored by proteasome inhibitors raises the attractive possibility that these mutant proteins may still be functional. Angelini *et al.*[30] did not find any of the RPS19 mutants that they studied in association with cytoplasmic ribosomes, even after proteasome inhibition. However, this experiment may be difficult to interpret since inhibition of the proteasome alters ribosome biogenesis by itself,[34] which may prevent efficient incorporation of the mutants into pre-ribosomes. In contrast, several class I RPS19 mutants with mutations equivalent to V15F and A62S were found to be incorporated into mature ribosomes and to partially complement shutdown of endogenous *RPS19* expression in yeast.[18,31] Although these mutations may have a weaker impact on yeast RPS19 when compared to the human protein, these results support the hypothesis that stabilized class I mutants could be functional.

## Authorship and Disclosures

AC performed all the experiments; LDC, JD, and AP analyzed the sequence of the *RPS19* gene; TL, LDC, GT and IM are in charge of the French DBA registry; OW-B provided the bortezomib reagent. CH, HM and VC performed cell culture and cell fractionation experiments; P-EG critically revised the manuscript; LDC directed the research work; NM and LDC designed the research, analyzed the data, and wrote the article. The authors reported no potential conflicts of interest.

## References


1. Diamond LK, Blackfan KD. Hypoplastic anemia. Am J Dis Child 1938; 56:464-7.
2. Josephs HW. Anaemia of infancy and early childhood. Medicine 1936; 15:307-451.
3. Willig TN, Niemeyer C, Leblanc T, Tiemann C, Robert A, Budde J, et al. Identification of new prognosis factors from the clinical and epidemiologic analysis of a registry of 229 Diamond-Blackfan anemia patients. Pediatr Res 1999;46:553-61.
4. Lutsch G, Stahl J, Kargel H, Noll F, Bielka H. Immunoelectron microscopic studies on the location of ribosomal proteins on the surface of the 40S ribosomal subunit from rat liver. Eur J Cell Biol 1990;51:140-50.
5. Draptchinskaia N, Gustavsson P, Andersson B, Pettersson M, Willig TN, Dianzani I, et al. The gene encoding ribosomal protein S19 is mutated in Diamond-Blackfan anaemia. Nat Genet 1999;21:169-75.
6. Gazda H, Grabowska A, Merida-Long LB, Latawiec E, Schneider HE, Lipton JM, et al. Ribosomal protein S24 gene is mutated in Diamond-Blackfan anemia. Am J Hum Genet 2006;79:1110-8.
7. Cmejla R, Cmejlova J, Handrkova H, Petrak J, Pospisilova D. Ribosomal protein S17 gene (RPS17) is mutated in Diamond-Blackfan anemia. Hum Mutation 2007;28:1178-82.
8. Farrar J, Nater M, Caywood E, et al. A large ribosomal subunit protein abnormalitity in Diamond-Blackfan anemia (DBA). Blood (ASH annual meeting abstracts) 2007; 110 [abstract].
9. Gazda HT, Sheen MR, Darras N, et al. Mutations of the genes for ribosomal proteins L5 and L11 are a common cause of Diamond-Blackfan anemia. Blood (ASH annual meeting abstracts). 2007;110 [abstract].
10. Willig TN, Draptchinskaia N, Dianzani I, Ball S, Niemeyer C, Ramenghi U, et al. Mutations in ribosomal protein S19 gene and Diamond-Blackfan anemia: wide variations in phenotypic expression. Blood 1999;94:4294-306.
11. Ball SE, McGuckin CP, Jenkins G, Gordon-Smith EC. Diamond-Blackfan anaemia in the U.K.: analysis of 80 cases from a 20-year birth cohort. Br J Haematol 1996;94:645-53.
12. Cmejla R, Blafkova J, Stopka T, Zavadil J, Pospisilova D, Mihal V, et al. Ribosomal protein S19 gene mutations in patients with Diamond-Blackfan anemia and identification of ribosomal protein S19 pseudogenes. Blood Cells Mol Dis 2000;26:124-32.
13. Matsson H, Davey E, Draptchinskaia N, Hamaguchi I, Ooka A, Levéen P, et al. Targeted disruption of the ribosomal protein S19 gene is lethal prior to implantation. Mol Cell Biol 2004; 24:4032-7.
14. Flygare J, Kiefer T, Miyake K, Utsugisawa T, Hamaguchi I, Da Costa L, et al. Deficiency of ribosomal protein S19 in CD34+ cells generated by siRNA blocks erythroid development and mimics defects seen in Diamond-Blackfan anemia. Blood 2005;105:4627-34.
15. Choesmel V, Bacqueville D, Rouquette J, Noaillac-Depeyre J, Fribourg S, Crétien A, et al. Impaired ribosome biogenesis in Diamond-Blackfan anemia. Blood 2007;109: 1275-83.
16. Flygare J, Aspesi A, Bailey JC, Miyake K, Caffrey JM, Karlsson S, et al. Human RPS19, the gene mutated in Diamond-Blackfan anemia, encodes a ribosomal protein required for the maturation of 40S ribosomal subunits. Blood 2007;109:980-6.
17. Liu JM, Ellis SR. Ribosomes and marrow failure: coincidental association or molecular paradigm? Blood 2006; 107:4583-8.
18. Léger-Silvestre I, Caffrey JM, Dawaliby R, Alvarez-Arias DA, Gas N, Bertolone SJ, et al. Specific role for yeast homologs of the Diamond Blackfan anemia-associated Rps19 protein in ribosome synthesis. J Bio Chem 2005;280:38177-85.
19. Da Costa L, Tchernia G, Gascard P, Lo A, Meerpohl J, Niemeyer C, et al. Nucleolar localization of RPS19 protein in normal cells and mislocalization due to mutations in the nucleolar localization signals in two Diamond Blackfan anemia patients: potential insights into pathophysiology. Blood 2003;101:5039-45.
20. Rouquette J, Choesmel V, Gleizes P-E. Nuclear export and cytoplasmic processing of precursors to the 40S ribosomal subunits in mammalian cells. Embo J 2005;24:2862-72.
21. Williams MS, Ettinger RS, Hermanns P, Lee B, Carlsson G, Taskinen M, et al. The natural history of

severe anemia in cartilage-hair hypoplasia. Am J Med Genet 2005; 138A:35-40.
22. Ridanpää M, van Eenennaam H, Pelin K, Chadwick R, Johnson C, Yuan B, et al. Mutations in the RNA component of RNase MRP cause a pleiotropic human disease, cartilage-hair hypoplasia. Cell 2001;104: 195-203.
23. Ridanpää M, Jain P, Mckusick VA, Francomano CA, Kaitila I. The major mutation in the RMRP gene causing CHH among the Amish is the same as that found in most Finnish cases. Am J Med Genet 2003;121C:81-3.
24. Williams MS, Hermanns P. Analysis of RPS19 in patients with cartilage-hair hypoplasia and severe anemia: preliminary results. Am J Med Genet 2005;138A:66-7.
25. Heiss NS, Knight SW, Vulliamy TJ, Klauck SM, Wiemann S, Mason PJ, et al. X-linked dyskeratosis congenita is caused by mutations in a highly conserved gene with putative nucleolar functions. Nat Genet 1998;19:32-8.
26. Luzzatto L, Karadimitris A. Dyskeratosis and ribosomal rebellion. Nat Genet 1998;19:6-7.
27. Woloszynek JR, Rothbaum RJ, Rawls AS. Mutations in SBDS gene are present in most patients with Shwachman-Diamond syndrome. Blood 2004;104:3588-90.
28. Austin KM, Leary RJ, Shimamura A. The Shwachman-Diamond SBDS protein localizes to the nucleolus. Blood 2005;106:1253-8.
29. Menne T, Goyenechea B, Sanchez-Puig N. The Shwachman-Bodian-Diamond syndrome protein mediates translational activation of ribosomes in yeast. Nat Genet 2007;39: 486-95.
30. Angelini M, Cannata S, Mercaldo V, Gibello L, Santoro C, Dianzani I, et al. Missense mutations associated with Diamond-Blackfan anemia affect the assembly of ribosomal protein S19 into the ribosome. Hum Mol Genet 2007;16:1720-7.
31. Gregory LA, Aguissa-Toure A-H, Pinaud N, Legrand P, Gleizes P-E, Fribourg S. Molecular basis of Diamond-Blackfan anemia: structure and function analysis of RPS19. Nucleic Acids Res 2007;35:5913-21.
32. Lam YW, Lamond AI, Mann M, Andersen JS. Analysis of nucleolar protein dynamics reveals the nuclear degradation of ribosomal proteins. Curr Biol 2007;17:749-60.
33. Andersen JS, Lam YW, Leung AK, Ong SE, Lyon CE, Lamond AI, et al. Nucleolar proteome dynamics. Nature 2005;433:77-83.
34. Stavreva DA, Kawasaki M, Dundr M, Koberna K, Müller WG, Tsujimura-Takahashi T, et al. Potential roles for ubiquitin and the proteasome during ribosome biogenesis. Mol Cell Biol 2006;26: 5131-45.